

## Quantum-Fluctuation-Initiated Coherence in Multioctave Raman Optical Frequency Combs

Y. Y. Wang,<sup>1</sup> Chunbai Wu,<sup>2</sup> F. Couny,<sup>1</sup> M. G. Raymer,<sup>2</sup> and F. Benabid<sup>1,\*</sup>

<sup>1</sup>*Gas-Phase Photonic Materials Group, CPPM, Physics Department, University of Bath, BA2 7AY, United Kingdom*

<sup>2</sup>*Department of Physics, Oregon Center for Optics, University of Oregon, Eugene, Oregon 97403, USA*

(Received 9 July 2010; published 15 September 2010)

We show experimentally and theoretically that the spectral components of a multioctave frequency comb spontaneously created by stimulated Raman scattering in a hydrogen-filled hollow-core photonic crystal fiber exhibit strong self-coherence and mutual coherence within each 12 ns driving laser pulse. This coherence arises in spite of the field's initiation being from quantum zero-point fluctuations, which causes each spectral component to show large phase and energy fluctuations. This points to the possibility of an optical frequency comb with nonclassical correlations between all comb lines.

DOI: 10.1103/PhysRevLett.105.123603

PACS numbers: 42.50.Ct, 42.50.Ar, 42.65.Dr, 42.65.Ky

Optical frequency combs play important roles in classical and quantum optics. In the classical case they enable the synthesis of ultrastable frequency references [1] and ultrashort optical pulses, the latter of which entails the production of a multioctave optical comblike spectrum of mutually coherent lines [2]. This is based either on high harmonic generation in noble gases [3] or high-order stimulated Raman scattering (SRS) from hydrogen [4,5]. In both processes, the medium coherence is externally driven so quantum vacuum fluctuations play no direct role in the comb generation.

SRS provides a unique juncture to explore the boundary between attosecond science and quantum optics. In SRS a microscopic quantum triggering event could be amplified to the macroscopic level. Early work on the statistical properties of SRS showed that when a spontaneously emitted Stokes field is excited by a quasi monochromatic single driving laser pulse, a macroscopic Stokes pulse is produced carrying with it signatures of its underlying quantum initiation in the forms of a Bose-Einstein-like probability distribution for photon number [4] and a uniform distribution of the random phase of the pulse [5]. Later it was discovered that when a Raman medium is excited by a single narrow-band laser pulse traveling in a hollow-core photonic crystal fiber (HC-PCF) containing hydrogen gas, a multioctave optical comb spectrum, spanning the near-IR to the near-UV, can be spontaneously generated by SRS with unparalleled efficiency [6].

The present study focuses on the quantum initiation of coherence in a Raman comb spontaneously created in H<sub>2</sub>-filled HC-PCF, and demonstrates for the first time an ultrawide comb containing coherence between lines that are generated purely from quantum-initiated vacuum noise fields, using a single narrow-band pump pulse. This single-pump-laser technique contrasts with the above-mentioned Raman excitation configurations [7–9], which rely on classically exciting the medium coherence by using multiple pump lasers or ultrashort pulsed lasers. We present direct experimental confirmation of the mutual coherence of the comb spectral lines and their quantum origin. We show that

comb lines have sufficient coherence to form correlated interference patterns. This was achieved by introducing a novel phase cross-correlator based on interfering independent Raman combs generated from two separate but identical Raman-scattering mediums. By comparing the fringes created simultaneously at two distinct comb frequencies, the results show a strong phase cross-correlation between any two spectral lines generated from a given Raman resonance within a single medium. These results, theoretically substantiated, contrast with previous works [4], showing that the quantum onset is due to spontaneously emitted light from a correlated pair of first-order Stokes (S1) and anti-Stokes (AS1) fields.

The quantum nature of the Raman comb initiation is demonstrated experimentally by the pulse-energy statistics of each spectral line from shot-to-shot, which exhibit the distinctive statistics of the vacuum field zero-point fluctuations. The duality of the lines' self-coherence (i.e. temporal and spatial coherence within a single-shot) and their super Poissonian photon statistics is attributed to the excitation condition whereby only a single vacuum spatial-temporal mode (STM) is amplified from the multimode vacuum field [10]. Furthermore, we show that the fluctuations of the S1 field are strongly correlated with those of the AS1 field. Such correlations would *not* be present in a truly thermal source; instead this shows that S1 and AS1 fields are part of a multimode squeezed state. This indicates the intriguing possibility of an optical comb spectrum creating attosecond pulses with nonclassical correlations (squeezing, entanglement) between the amplitudes and phases of all comb lines.

Figure 1(a) shows the interferometric setup used to measure the mutual coherence and the pulse-energy statistics of the comb components. Two 70-cm pieces of identical H<sub>2</sub>-filled HC-PCF [6,11] are excited with equal optical power from a single-frequency Nd-YAG laser to separately and independently generate a series of higher-order Raman spectral components. The laser emits 12 ns-long, nearly transform-limited pulses at 1064 nm with 50-Hz repetition rate. The HC-PCF used is a large-pitch

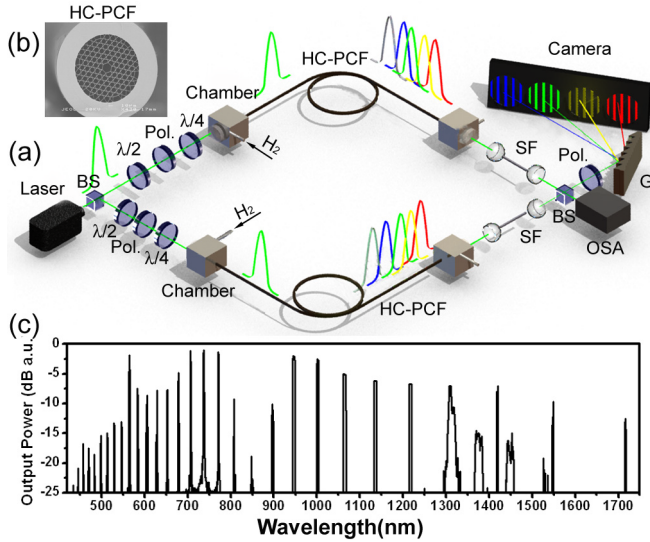


FIG. 1 (color online). (a) Interferometer with  $H_2$ -filled HC-PCF [shown in (b)] in each arm. SF: spatial filter, BS: beam splitter, OSA: optical spectrum analyzer, Pol: polarizer,  $\lambda/2$ : half-wave plate,  $\lambda/4$ : quarter-wave plate, G: grating. (c) Output power spectrum from one fiber.

single-cell Kagome fiber [6] with a  $30 \mu\text{m}$  hollow core [Fig. 1(b)]. The fiber dominantly guides a polarization-degenerate  $HE_{11}$ -like core mode. A grating is used to separate the Raman spectral pairs of the combined beam at the output of the interferometer, and spectral pairs are sent to a CCD camera and recorded on a single-shot basis. The typical output spectrum from each HC-PCF is shown in Fig. 1(c) when the fiber is excited by  $\sim 30 \text{ mW}$  of average pump power. The spectral comb spans from below  $400 \text{ nm}$  to above  $1750 \text{ nm}$ . The spectral components consist of S and AS lines spaced by  $\sim 125 \text{ THz}$  for those raised from the vibrational  $S_{00}(1)$  transition and by  $\sim 18 \text{ THz}$  for those raised from the rotational  $Q_{00}(1)$  [6].

Figure 2(a) shows single-shot profiles of the interferograms from the pump pair at  $1064 \text{ nm}$  and of four degenerate spectral pairs from the two fibers at wavelengths  $740$ ,  $770$ ,  $1003$ , and  $1134 \text{ nm}$ . The comb-line spatial interferograms exhibit deep interference fringes, indicating a strong “self-coherence” of each Raman line. Such interference occurs for every pair of comb components. Self-coherence arises from the transiency of the Raman process [5], which in HC-PCF, due to the ultrahigh Raman gain, can occur even with a pump pulse as long as  $12 \text{ ns}$  [12]. In this high-gain transient regime, the number of STM (coherent wave packets) of the vacuum-initiated Stokes field that are amplified to the macroscopic level is reduced to one [10], which exhibits a constant random phase throughout its duration.

The quantum nature of the comb onset was investigated by measuring the statistical distributions of the fringe visibility and of the relative phase of each degenerate pair of comb lines from the two fibers. Figs. 2(b)–2(e) show the results of four representative line pairs for 150

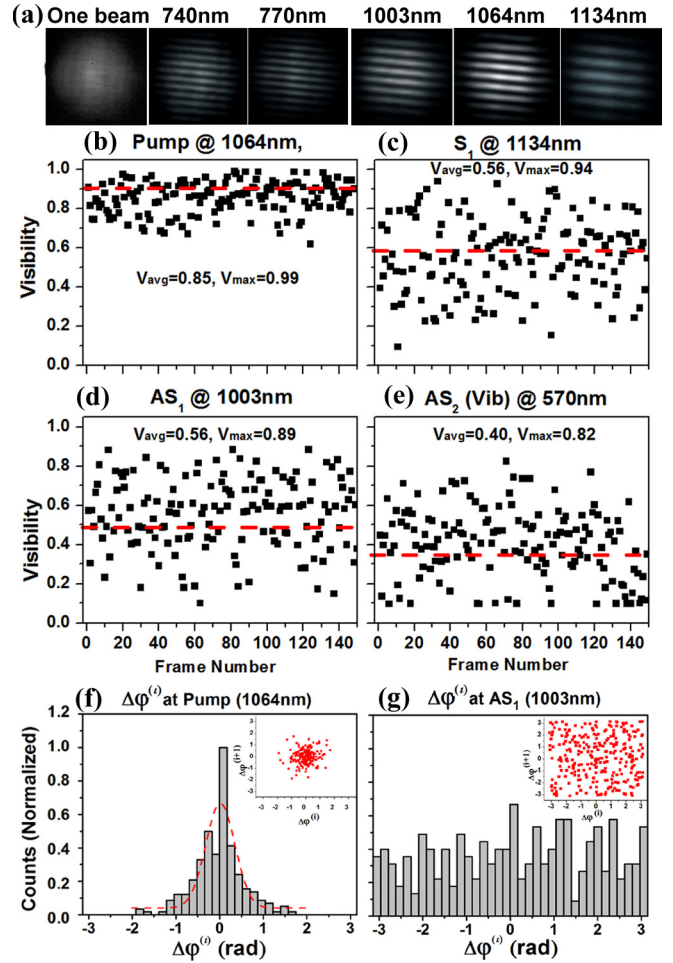


FIG. 2 (color online). (a) Mode pattern for one interferometer arm at  $740 \text{ nm}$  (far left), and (other panels) when two arm beams at the indicated wavelengths are combined. Shot-to-shot visibilities and phase distributions. (b)–(e) Visibilities of line-pairs from 150 different pump shots of the pump (b); two rotational (c),(d) and a vibrational component (e). (f),(g) Phase histograms of the pump (f) and the first rotational  $AS_1$  fields (g).

pump shots. For all data, we used pump pulses having the same average power ( $\sim 30 \text{ mW}$ ) within a 1% range in order to reduce the effects of pump power fluctuations. The long separation between the pulses ( $20 \text{ ms}$ ) ensures that the STM excited by each successive pump pulse are uncorrelated. Each CCD frame corresponds to a single shot of the pump laser. The visibility of each interferogram is extracted by normalizing it with the beam profile of the Raman lines for each pulse and fitting to a sine function. The fit also gives the shot-to-shot relative phase between different interferograms  $\Delta\varphi^{(i)} = \varphi^{(i+1)} - \varphi^{(i)}$ . The superscript  $(i)$  indicates the shot number or equivalently the frame number. Figs. 2(b) and 2(f) show the shot-to-shot distributions of the visibility and phase of the transmitted pump. They both exhibit narrow distributions typical of coherent light, although the phase distribution is broadened by interferometer jitter. The measured visibility has an average of  $0.85$  and small standard deviation. Similarly,

the phase exhibits a Gaussian distribution with a half-width-at-half-maximum of 0.78 rad and a phase portrait concentrated near the center [inset of Fig. 2(f)].

In contrast, and despite exhibiting self-coherence, the higher-order Raman lines show a strongly fluctuating visibility, as illustrated by three representative components: rotational S1 at 1134 nm, AS1 at 1003 nm and the vibrational AS2 lines [Figs. 2(c)–2(e)]. The visibility fluctuates from near 0 to 0.94, with an average visibility of 0.40 to 0.56. The measured average visibilities are in fair agreement with the theoretical prediction for two spatially coherent, monochromatic, thermal pulses interfering, which theoretically yields a mean visibility of  $\pi/4 = 0.78$  [4].

The phase distributions were found to be uniform for all measured S and AS lines, as illustrated by the histogram of  $\Delta\varphi^{(i)}$  for AS1 at 1003 nm in Fig. 2(g). The observed shot-to-shot fluctuations of the visibility and phase indicate the underlying quantum nature of the S and AS lines.

While the above results indicate the quantum nature of the triggering process of the comb, they do not provide information on the phase correlation (i.e., mutual coherence) between comb lines within each pulse. To that end, we observed the relationship between the fringe phases arising from a given line pair (e.g., S1 and AS1) on each shot. Correlation of these fringe phases implies correlation between lines from within a single comb. We create phase-correlation histograms by simultaneously recording interferograms of several Raman pairs within a single CCD frame. This is illustrated in Fig. 3(a), which shows the interferograms for the pump P, the rotational S1, AS1, and AS2 lines for a given shot. Such a technique allows extracting any underlying phase relationship between any two spectral components.

In our case, as explained below, the theoretically expected phase relationship between the lines is  $\varphi_n = n\varphi_{\text{QF}} + \delta_n$  [6]. Here  $\delta_n$  is a deterministic phase shift that arises from the pump-laser or fiber-propagation-in-

duced phase noise and any dynamical phase shifts from the amplification process, and  $n$  is the order of the Raman lines (negative for Stokes and positive for anti-Stokes lines).  $\varphi_{\text{QF}}$  is the resultant phase of the collective, coherent state of the molecular excitations, determined by amplification of quantum fluctuations [13], and is constant throughout a single pulse. Consequently, the phase difference for comb lines  $m$  and  $n$ , defined as  $m\varphi_n - n\varphi_m = m\delta_n - n\delta_m$ , is predicted to be approximately constant.

The phase relationship mentioned above stems from the quantum propagation theory, which is based on the equations of motion for the electric-field operators  $E_n^{(-)}$  of each comb line denoted by integer  $n$  and the collective molecular vibration raising operator  $P$  of the group of molecules located at position  $z$ :

$$\begin{aligned} \partial_z E_n^{(-)}(z, \tau) &= -i\alpha_{2,n+1} E_{n+1}^{(-)} \exp(-i\Delta\beta_{n+1}z) P^\dagger \\ &\quad - i\alpha_{2,n}^* E_{n-1}^{(-)} \exp(i\Delta\beta_n z) P, \\ \partial_\tau P^\dagger(z, t) &= i \sum_{n=-N}^N \alpha_{1,n} E_n^{(+)} E_{n-1}^{(-)} \exp(i\Delta\beta_n z) - \Gamma P^\dagger + F_\Gamma. \end{aligned}$$

Here,  $\alpha_{1,n}$  and  $\alpha_{2,n} = 2\pi\hbar N\omega_n \alpha_{1,n}^*/c$  are complex interaction coefficients,  $\Delta\beta_n = \beta_n - \beta_{n-1}$  is the difference between propagation constants of adjacent Raman lines, and  $F_\Gamma$  and  $\Gamma$  are the quantum Langevin operator and damping rate associated with molecular collisions. The initial conditions for these operators are those of standard quantum noise [6,14,15]. We consider the case where only first-order Stokes  $E_{-1}$  and anti-Stokes  $E_{+1}$  fields are excited, and the pump intensity profile is unchanged throughout the interaction. This model allows us to find a full quantum description and gain insight into the comb generation process. In the high-gain, transient regime we can neglect the Langevin operator and damping. The analytic form of solutions can be found using the methods in [15,16], and take an analytic form:

$$\begin{pmatrix} E_{-1}^{(-)}(L, \tau) \\ E_{+1}^{(+)}(L, \tau) \end{pmatrix} = -E_0(\tau) \int_0^L d\tilde{z} \begin{pmatrix} i\alpha_{2,-1} G_{13}(\tilde{z}, \tau) \\ -i\alpha_{2,1} G_{23}(\tilde{z}, \tau) \end{pmatrix} P^\dagger(\tilde{z}, 0) + E_0(\tau) \int_0^\tau d\tilde{\tau} E_0(\tilde{\tau}) \begin{bmatrix} \alpha_{2,-1} G_{11} & \alpha_{2,-1} G_{12} \\ -\alpha_{2,1} G_{21} & -\alpha_{2,1} G_{22} \end{bmatrix} \begin{pmatrix} E_{-1}^{(-)}(0, \tilde{\tau}) \\ E_{+1}^{(+)}(0, \tilde{\tau}) \end{pmatrix},$$

where the Green propagators are known functions [17]. The nonzero off-diagonal elements of the Green matrix show that the two fields are components of a squeezed state.

Figure 3(b) shows the calculated mean intensity profiles of the pump and rotational S1 and AS1 components for the experimental conditions, but assuming only S1 and AS1 fields are generated. They are seen to grow simultaneously. More importantly, Fig. 3(b) shows that the S1 and AS1 fields are predicted to have perfect phase anticorrelation, with a near-unity correlation coefficient  $C$  throughout the pulse duration, which is defined by  $|\langle E_{-1}^{(-)}(L, \tau) E_{+1}^{(-)}(L, \tau) \rangle| / \sqrt{\langle E_{-1}^{(-)}(L, \tau) E_{-1}^{(+)}(L, \tau) \rangle \langle E_{+1}^{(-)}(L, \tau) E_{+1}^{(+)}(L, \tau) \rangle}$  [17].

The predicted correlations between S1 and AS1 fields are experimentally confirmed in Fig. 3(c). It shows the phase-difference histogram from 250 successive shots, with Gaussian fits centered at 0, of the first S and AS pair of the rotational Raman resonance, along with the observed shot-to-shot intensity correlation between S1 and AS1 fields [Fig. 3(c) inset]. To quantify the phase correlation between the  $n$ -order and  $m$ -order Raman lines; the phase axis of the histogram is defined as  $\Phi_{nm} = m\Delta\phi_n^{(i)} - n\Delta\phi_m^{(i)}$ , where  $\Delta\phi_n^{(i)} \equiv \Delta\varphi_n^{(i+1)} - \Delta\varphi_n^{(i)}$ , and  $\Delta\varphi_n^{(i)}$  is the extracted fringe phase of the  $i$ th laser shot and the  $n$ -order Raman line. This was evaluated by extracting interference fringe phase difference  $\Delta\varphi_n^{(i)} = \varphi_{n,1}^{(i)} - \varphi_{n,2}^{(i)}$ , with 1 and 2 denoting individual fibers. Consequently, under the ideal-

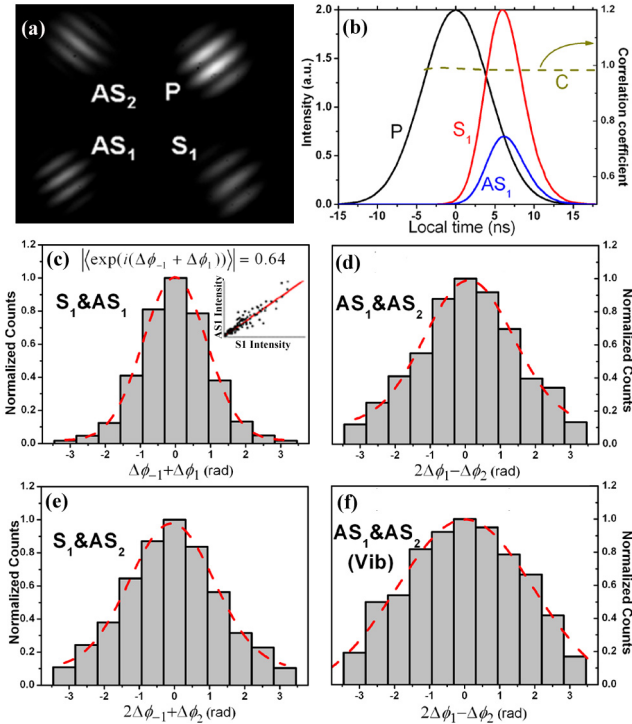


FIG. 3 (color online). Results for mutual coherence experiment. (a) interferograms of four different Raman orders in a single frame. (b) Calculated temporal profile of mean pulse intensities of the pump (P), S1 and AS1 fields as a function of local time when phase mismatch  $(2\beta_p - \beta_S - \beta_{AS})L$  equals the experimental value 30. Curve C is the Stokes-anti-Stokes correlation coefficient, based on the quantum theoretical model (see text). (c) Measured histogram of phase-difference for rotational AS1 and S1 fields, with Gaussian fit. Inset is the shot-to-shot intensity relation of the two lines. (d)–(f) Histograms of phase difference for (d) Rt-AS-2 and Rt-AS-1; (e) Rt-AS-2 and Rt-S-1; (f) Vb-AS-1 and Vb-AS-2.

ization of perfect phase correlations, the above fringe phase can be rewritten as  $\Delta\varphi_n^{(i)} = n\varphi_{\text{QF},1}^{(i)} + \delta_{n,1} - (n\varphi_{\text{QF},2}^{(i)} + \delta_{n,2}) \equiv n\Delta\varphi_{\text{QF}}^{(i)} + \Delta\delta$ . The quantity  $\Delta\varphi_n^{(i)}$  is defined above as the phase difference of two successive shots in order to cancel the deterministic phases  $\delta_n$ .

The observed peaking of the distribution around zero unambiguously indicates the presence of strong phase correlation. This is quantified by the ensemble-averaged correlation coefficient  $|\langle \exp(i\Phi_{nm}) \rangle|$ , which was found to be 0.64. Writing  $I_{\pm 1} = \langle E_{\pm 1}^{(-)} E_{\pm 1}^{(+)} \rangle$ , this phase-correlation coefficient is directly proportional to the degree of mutual phase coherence  $|\langle \exp(i\Phi_{1,-1}) \rangle|$ , as is seen from  $C = |\langle |E_{-1}^{(-)}| |E_{+1}^{(-)}| \rangle| (I_{-1} I_{+1})^{-1/2} \langle e^{-i(\varphi_{-1} + \varphi_{+1})} \rangle|$ , valid if we assume that the fluctuations in intensities  $|E_{\pm 1}^{(-)}|^2$  of S1 and AS1 fields are independent of that of their phases. The relatively smaller value 0.64 of the correlation coefficient observed for S1 and AS1 fields [Fig. 3(c)] indicates that when many lines are generated, the comb dynamics are more complicated than accounted for by the idealized model, which predicts a value near 1. The observed posi-

tive correlation of S and AS intensities [Fig. 3(c) inset] along with anticorrelation of their phases is consistent with the behavior of a nonclassical two-mode squeezed state.

Moreover, the mutual coherence is found to be present for any other spectral line pair from a given Raman resonance, as is illustrated by the phase-correlation histograms of the rotational pairs AS1-AS2 [Fig. 3(d)] and S1-AS2 [Fig. 3(e)], or the vibrational AS1-AS2 pair [Fig. 3(f)]. These correlations follow the general relation  $\varphi_n = n\varphi_{\text{QF}} + \delta_n$ , mentioned above. The origin of this correlation of higher-order lines is well explained by a new self-consistent theoretical model [17]. It shows that during the onset of S1 and AS1 fields, the medium polarization is driven in the same manner as a phase modulator to generate the higher-order Raman sidebands. Because the S1 and AS1 pair acts like a pump to generate the comb through the parametric process of phase modulation, all the higher-order components should be correlated in a manner similar to the correlation of S1 and AS1 fields.

This work has shown that an optical frequency comb spectrum spanning from the UV to the mid-IR can be spontaneously created containing a high degree of quantum coherence among comb lines, without introducing any macroscopic coherence into the system from external sources. This opens the possibility to explore generating isolated pulses in the attosecond regime having nonclassical properties such as reduced noise via quantum-state squeezing.

This work is supported by UK EPSRC grant EP/E039162/1 and US NSF grant PHY-0757818.

\*Corresponding author.

f.benabid@bath.ac.uk

- [1] J. L. Hall, *Rev. Mod. Phys.* **78**, 1279 (2006).
- [2] M. Hentschel *et al.*, *Nature (London)* **414**, 509 (2001).
- [3] E. Goulielmakis *et al.*, *Science* **320**, 1614 (2008).
- [4] I. A. Walmsley and M. G. Raymer, *Phys. Rev. Lett.* **50**, 962 (1983).
- [5] S. J. Kuo, D. T. Smithey, and M. G. Raymer, *Phys. Rev. A* **43**, 4083 (1991).
- [6] F. Couny *et al.*, *Science* **318**, 1118 (2007).
- [7] M. Y. Shverdin *et al.*, *Phys. Rev. Lett.* **94**, 033904 (2005).
- [8] A. V. Sokolov *et al.*, *J. Mod. Opt.* **52**, 285 (2005).
- [9] P. J. Bustard, B. J. Sussman, and I. A. Walmsley, *Phys. Rev. Lett.* **104**, 193902 (2010).
- [10] M. G. Raymer, I. A. Walmsley, and E. Wolf, in *Progress in Optics* (Elsevier, New York, 1990), p. 181.
- [11] F. Benabid *et al.*, *Science* **298**, 399 (2002).
- [12] F. Benabid *et al.*, *Phys. Rev. Lett.* **95**, 213903 (2005).
- [13] D. T. Smithey *et al.*, *Phys. Rev. Lett.* **67**, 2446 (1991).
- [14] J. R. Ackerhalt and P. W. Milonni, *Phys. Rev. A* **33**, 3185 (1986).
- [15] S. Y. Kilin, *Europhys. Lett.* **5**, 419 (1988).
- [16] M. G. Raymer and J. Mostowski, *Phys. Rev. A* **24**, 1980 (1981).
- [17] C. Wu, M. G. Raymer, Y. Y. Wang, and F. Benabid, *Phys. Rev. A* (to be published).